FAPI Controller for Frequency Support in Low-Inertia Power Systems

Rakhshani, Elyas; Perilla , Arcadio; Rueda Torres, José L. ; Gonzalez-Longatt, Francisco M.; Soeiro, Thiago Batista; van der Meijden, M.A.M.M.

DOI
10.1109/OAJPE.2020.3010224

Publication date
2020

Document Version
Final published version

Published in
IEEE Open Access Journal of Power and Energy

IEEE Open Access Journal of Power and Energy

Received 24 April 2020; revised 22 June 2020; accepted 12 July 2020. Date of publication 20 July 2020; date of current version 31 July 2020.

Digital Object Identifier 10.1109/OAJPE.2020.3010224

FAPI Controller for Frequency Support in Low-Inertia Power Systems

ELYAS RAKHSHANI[1] (Member, IEEE), ARCADIO PERILLA[1], JOSÉ L. RUEDA TORRES[1] (Senior Member, IEEE), FRANCISCO M. GONZALEZ-LONGATT[2] (Senior Member, IEEE), THIAGO BATISTA SOEIRO[1] (Senior Member, IEEE), AND MART A. M. M. VAN DER MEIJDEN[1,3] (Member, IEEE)

[1]Department of Electrical Sustainable Energy, Delft University of Technology, 2628 CD Delft, The Netherlands
[2]Department of Electrical Engineering, Information Technology and Cybernetics, University of South-Eastern Norway, 3679 Notodden, Norway
[3]TenneT TSO B.V., 6800 AR Arnhem, The Netherlands

CORRESPONDING AUTHOR: E. RAKHSHANI (elyas.rakhshani@gmail.com)

This work was supported in part by the MIGRATE Project, and in part by the European Union's Horizon 2020 Research and Innovation Program under Grant 691800.

ABSTRACT This paper presents different forms of Fast Active Power Injection (FAPI) control schemes for the analysis and development of different mitigation measures to address the frequency stability problem due to the growth of the penetration level of the Power Electronic Interfaced Generation (PEIG) in sustainable interconnected energy systems. Among the studied FAPI control schemes, two different approaches in the form of a derivative-based control and a virtual synchronous power (VSP) based control for wind turbine applications are also proposed. All schemes are attached to the PEIG represented by a generic model of wind turbines type 4. The derivative-based FAPI control is applied as an extension of the droop based control scheme, which is dependent on the measurement of the network frequency. By contrast, the proposed VSP-based FAPI is fed by the measurement of the active power deviation. Additionally, unlike existing approaches for virtual synchronous machines, which are characterized by high-order transfer functions, the proposed VSP-based FAPI is defined by a second-order transfer function, which can contribute to fast mitigation of the system primary frequency deviations during containment period. The Great Britain (GB) test system, for the Gone-Green planning scenario for the year 2030 (GG2030), is used to evaluate the effects of the proposed FAPI controllers on the dynamics of the system frequency within the frequency containment period. Thanks to proposed FAPI controllers, it is possible to reach up to 70% for the share of wind power generation without violating the threshold limits for frequency stability. For verification purposes, a full-scale wind turbine facilitated with each FAPI controller is tested in EMT real-time simulation environment.

INDEX TERMS Frequency stability, fast active power injection, virtual inertia, inertia emulation, MIGRATE project, wind power integration, energy storage, low-inertia system.

I. INTRODUCTION

THE frequency of interconnected systems can deviate from its scheduled values when the network is exposed by different types of contingencies, e.g. the sudden loss of a generation unit and/or a large increment of power demand. In low-inertia power systems that suffer from sufficient inertia and governor headroom, the system might experience a large frequency excursion with unacceptable values for Rate of Change of Frequency (RoCoF) and Nadir [1]–[4]. The main concern with power electronic-based generation units is that they cannot wholly replace the inertial effect of conventional generators. Therefore, this results in the system frequency being more volatile [5]–[10]. As shown in [11], thanks to advanced control methodologies, wind generators can attempt to have dynamic behavior like synchronous generators (SG) during the frequency containment period. However, this functionality has its limitations due to technology challenges that constrain the physical size of the currently

available wind generators. Furthermore, the intermittency of this type of renewable-based generation unit might also worsen the system response. This calls for new additional solutions such as the embedded energy storage systems, and complementary control actions for facilitating Fast Frequency Response (FFR) [12]–[14].

A well-designed Inertia Emulation (IE) controller empowers the wind generator, or storage element, to release the stored energy for arresting the frequency drop within 10.0 seconds [15]–[18]. Fast frequency controllers can be classified in three main families, namely, droop-based controllers (or proportional controllers) [19]–[21], derivative-based controllers [22]–[24], and other approaches which are usually based on the swing equation of conventional SG, thus attempting to represent a Virtual Synchronous Machine (VSM) for IE [25], [26].

Given the existing literature, the methods based on the droop control are easy to implement and may allow achieving good damping with an acceptable frequency recovery time. Thus their main improvement will be on Nadird value and not in the ROCOF [19], [20]. In contrast, the derivative control can impact the value of ROCOF and different researches have also reported that by means of derivative-based control alone, the first peak of frequency response can significantly be improved while the frequency recovery might be limited following an active power imbalance [19], [20]. In the case of wind power application, if the derivative-based controller reverses the direction of the power, modification of power reference due to control action, the signal after the frequency reaches its limit value, the wind turbine will require additional control actions to recover to its optimum operating condition. In this case, additional droop based control is used as a complementary control action to produce a change in the power reference, extracted wind power, in proportion to the system frequency deviation. Therefore, a combination of different methods like proportional (droop) and derivative controls seems to be an effective solution [27]–[30].

In this paper, for suppressing the primary frequency response especially during the containment period, different forms of FAPI control schemes with two new propositions are presented and discussed. These are implemented in the form of a derivative-based FAPI control and a virtual synchronous power (VSP)-based FAPI controller. As it will be explained in the paper, FAPI is a mechanism that can rapidly adjust the injection/absorption of active power to efficiently alleviate the deviations of the frequency in a highly penetrated network. The primary source of stored energy to emulate virtual inertia is in other systems interfaced by power electronic circuits, like battery banks and mechanical rotating components in the wind generator.

The contribution of this paper resides in several aspects as follows:

- The proposed FAPI controllers are designed and configured for wind power type 4 generation units. The proposed control scheme is preformed considering a wind park controller with full details in the DIgSILENT platform. The proposed derivative-based FAPI controller is realized as an extension of the droop based approach, which is dependent on the measurement of the network frequency. By contrast, the proposed VSP-based FAPI is fed by the measurement of the active power deviation. Additionally, unlike existing approaches related to the implementation of virtual synchronous machines, which are typically characterized by high-order transfer functions, the proposed VSP-based FAPI is defined by a second-order transfer function. It will be shown that this can contribute to the fast mitigation of the system frequency deviations without limitations from the Phase-Locked-Loop (PLL).
- Another novelty of this paper is related to the proposition of a sensitivity-based method for tuning the FAPI controller. This methodology is based on time-domain simulations which can be easily implemented by the system operator. This part is done for evaluating the impact of the FAPI's control parameters on the dynamics of the system's frequency within the containment period.
- Most of the existing researches found in the literature which works on FAPI is focused on controller designs considering a single or a small set of wind generators. Additionally, the studied systems are usually connected to a relatively low capability or small-size network. Nevertheless, a comprehensive methodology to assess the effects of the FAPI control parameters of the wind generators which are facilitated by the FAPI controller is required to define the maximum penetration of PEIG that does not bring any risk for the frequency instability. This gap has been also addressed in this paper.
- Lastly, for considering the effects of the various penetration level of the wind generation, the GB test system is also incorporated for verifying the performance of the designed mitigation measures. In the studied GB system, the operational scenarios of the Gone Green (GG) initiative for 2030 are derived based on the ten years planning perspective [30].
- For testing and validation of the proposed FAPI methods, EMT real-time simulations are also performed to examine the implications on the generator and converters of a wind power generator type 4.

The remainder of the paper is organized as follows: the used power system benchmarks and the Wind Generator (WG) control schematic with its integrated structure are presented in Section II. Details of the proposed FAPI controller and implementation of different control laws for FAPI are presented and discussed in Section III. The proposed methodology for a sensitivity-based analysis for tuning and determination of the maximum share of wind generation is discussed in Section IV. In Section V, the use of the proposed FAPI controller on the GB test system is studied and compared with other control approaches. Finally, the test validation and concluding remarks are presented in Sections VI and VII, respectively.

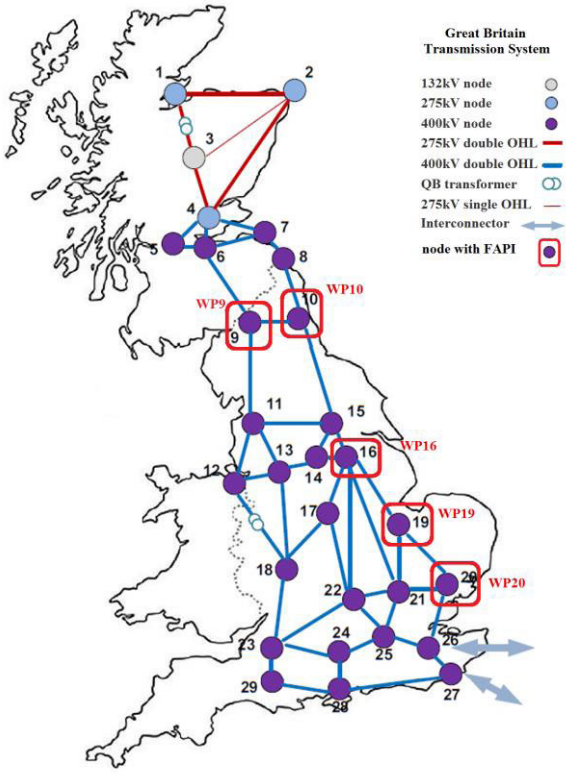

FIGURE 1. **GB test system (WP stands for wind park).**

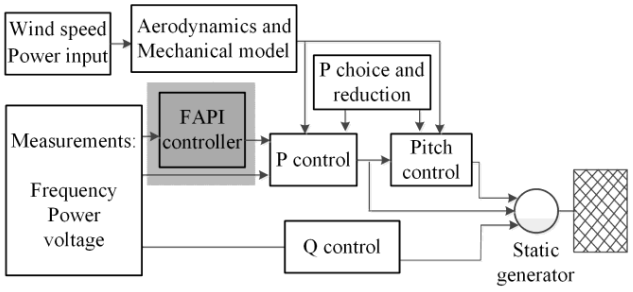

FIGURE 2. **The control structure for the Type-4 wind generator.**

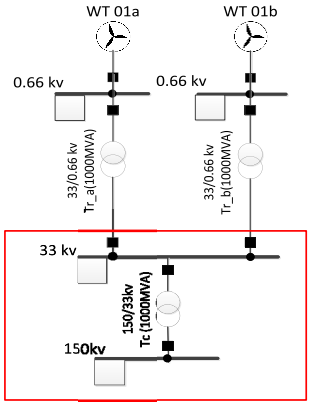

FIGURE 3. **Grid-interface of a wind park with two types of WGs.**

II. STUDIED OPERATIONAL SCENARIO

A. GB TEST SYSTEM

This paper uses the GB test system model developed in the works [31], [32]. Figure 1 shows that the used GB test network consists of 29 zones where each of them consists of a clustered level of generation units, load, and grid losses.

To study the future transition scenarios in the GB network, one of the extreme scenarios called 'Gone Green' has been chosen. The Gone Green scenario intended to investigate the maximum share of wind power migration [32]. The main studied setting is the one defined by the Gone Green scenario in the year 2030 (GG2030) with the penetration ratio of up to 78%.

B. WIND POWER INTEGRATION AND CONTROL

The WG model is implemented according to the standards of the IEC 61400-27 series [21].

As shown in Figure 2, different blocks that represent modifications in respect to the IEC standard with a brief explanation of their roles are presented [21]. The key aspects of the studied model are explained as follows:

- In the measurement section of this model, the measurement blocks for Frequency, Power, and Voltage have a direct connection to the WG terminals.

- The Generator block consists of the 'Static Generator' from PowerFactory elements. The details of the Generator block are based on the IEC 61400-27-1 standard [33].

- The Aerodynamic block is used for the representation of the mechanical parts of the wind generation unit [34].

- The input block contains wind speed and power inputs. The wind speed is provided by using an external file with wind speed measurements in meter per second (m/s).

- The P control and Pitch angle controller blocks are built according to [34]. The ''FAPI controller'' block, shown in light grey in Figure 2, is an additional block to the developed wind generation model. Depending on the applied control strategy within the FAPI, its input signal can be the measured power or frequency. While the output signal is the supplementary reference to the active power control for fast active power injection capabilities.

As shown in Figure 3, a wind park is implemented which can be used for representing the connection of various feeders with wind generations.

III. FAPI BASED CONTROLLER FOR INERTIA EMULATION

A. CONVENTIONAL APPROACH: DROOP BASED FAPI CONTROLLER

If In this paper, for adding the capability of IE to the WG control structure, a precise droop-based control approach is implemented. The general structure of the implemented droop-based FAPI control is shown in Figure 4. It creates a droop-based inertia emulation implemented inside of the FAPI block in the WG model (shown in Figure 2). The FAPI

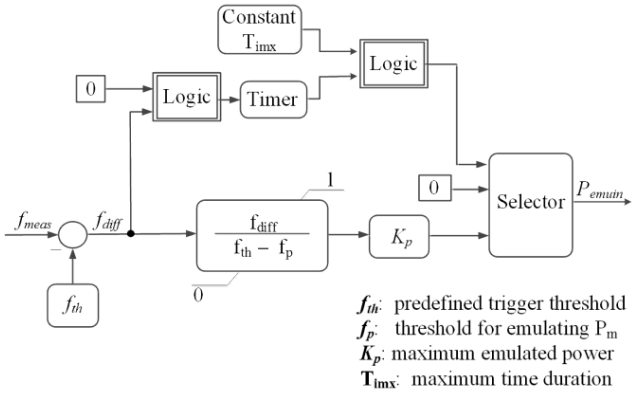

FIGURE 4. **Implemented inertial emulation block with droop-based control.**

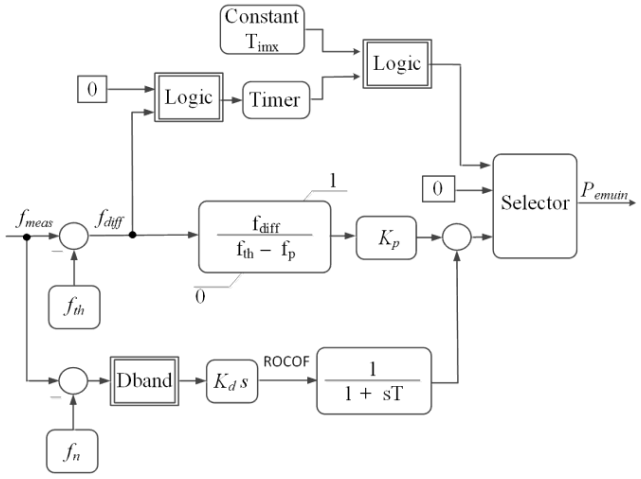

FIGURE 5. **Block diagram of the derivative plus droop based FAPI controller.**

controller can react to a drop in the grid frequency with a temporary increase in the active power output of the wind generator.

The main control parameters of this FAPI controller that affect the dynamic response during activation of the controller are: (i) the activation threshold for the FAPI controller (f_{th}), (ii) the maximum duration of FAPI activation (T_{imx}), (iii) the threshold for maximum emulated power (f_p) and (iv) the allowable additional power output (K_p). The value of f_{th} is assumed to be equal to 49.90 Hz. In case the frequency reaches an even lower value, corresponding with a second threshold f_p, then, the maximal allowed power through emulated inertia is released.

In droop-based control, according to the value defined for the proportional gain K_p, there will be a linear dependency between deviations of the grid frequency from its reference value (50Hz / 60Hz) and the surplus reference power (P_{emuin}). The following equation is used for this purpose:

$$P_{emuin}\,(\mathrm{t}) = \frac{f_{th} - f_{meas}\,(\mathrm{t})}{f_{th} - f_p} K_p \tag{1}$$

According to [29], the value of the proportional gain K_p could be set around 20% of the rated active power of the WG. Thus, following the logic shown in Figure 4, in case the measured frequency goes up to f_{th} or if the total allowed duration of IE (T_{imx}) is reached, then the FAPI will be deactivated by selecting a zero gain as the output reference power, P_{emuin}, of the controller.

The time duration for the FAPI controller, T_{imx}, is determined based on the logic used in the upper loop of the designed controller in Figure 4. A constant value for the T_{imx} can be selected by a user. Then, by adding a timer block and a selector (as shown in Figure 4), the FAPI controller can be deactivated (by switching the output to zero) as soon as the T_{imx} is reached. According to [21] and [35], [36], T_{imx} can vary from 5 s to 25 s. During this period of time, different sources can be used for providing inertia. The mechanical part of a wind turbine is not the only source and different options like stored energy in DC link (Embedded capacitors) are also good candidates for providing energy.

B. PROPOSITION 1: DERIVATIVE BASED FAPI CONTROLLER

In this control technique, the task of fast active power injection is performed by using the derivative term of the system frequency. This action can be done by adjusting the reference of the active power controller of the converter:

$$\Delta P_{emuin} = -k_d \frac{\mathrm{d}(\Delta f)}{\mathrm{d}t} \tag{2}$$

This control consists of a derivative function and controller gain for emulating the desired portion of inertia. Since the derivative-based control might cause amplification on the measurement noise, a low-pass filter is considered. In addition to the noise amplification, the calculation time needed in digital data processing to calculate the derivative term might introduce additional delay. As shown in Figure 5, the implemented derivative-based FAPI is performed by adding an additional control loop. In this control, the new parameters are the derivative gain (K_d) and the filter time constant (T).

It is considered that the wind generator operates close/lower than its MPPT value, therefore, in addition to DC-link energy, there is enough power that can be extracted during the frequency containment period. It is assumed that wind turbines can be operated up to 10%-15% above the rated power. Thus, wind generation can be dispatched in a way that it can have more headroom during normal operating conditions [11].

C. PROPOSITION 2: VSP BASED FAPI CONTROLLER

Figure 6 presents the general structure of the ultimate controller, the VSP-based FAPI controller, for emulating inertial droop response and damping of a normal SG. The structure of this controller is coming from suitable programming of the electrical performance of a conventional SG on a digital

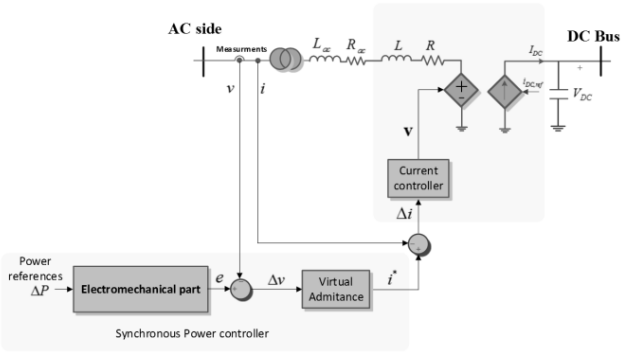

FIGURE 6. **The general control structure of VSP-based control of a VSC.**

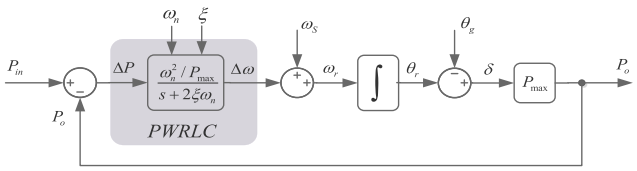

FIGURE 7. **Electromechanical representation of the VSP control.**

basis that is taking care of controlling the VSC converter. Depending on the converter technology, an additional source of energy, like storage elements, can be added into the DC side of a VSC station.

The VSP is located in the outer-loop control of the VSC, providing a power reference for the inner loop (current) controller. Figure 7 shows the control diagram of the VSP strategy. This figure implies a control approach, in which differences between the measured output power of the converter (P_o) and the input (reference) power (P_{in}) is managed with a block called Power Loop Controller (PWRLC) for setting a virtual frequency which has to be added to the grid's frequency (ω_s), for creating the rotating frequency of a virtual rotor (ω_r). The integration of such virtual frequency will give the angular position of the virtual rotor, which corresponds to the phase angle of the induced *emf* in the virtual stator, which enables power injection like in the inertial response of an SG. The difference between the phase-angle of the induced voltage, θ_r, and the phase-angle angle of the grid voltage, θ_g, gives the load angle, δ, which allows calculating the power delivered by the power converter. The representation of the PWRLC in the VSP controller has a second-order characteristic, which makes it possible to simultaneously impact the damping (k) and the inertia (J) of the system.

The dynamic relations between the input and the output power of the presented VSP can be lead to the following second-order equation:

$$\frac{P_o}{P_{in}} = \frac{\omega_n^2}{s^2 + 2\zeta\omega_n s + \omega_n^2} = \frac{\frac{P_{max}}{J.\omega_s}}{s^2 + \frac{k}{J.\omega_s}s + \frac{P_{max}}{J.\omega_s}} \tag{3}$$

where ζ and ω_n are the damping factor and natural frequency, respectively. While the P_{max} is the maximum

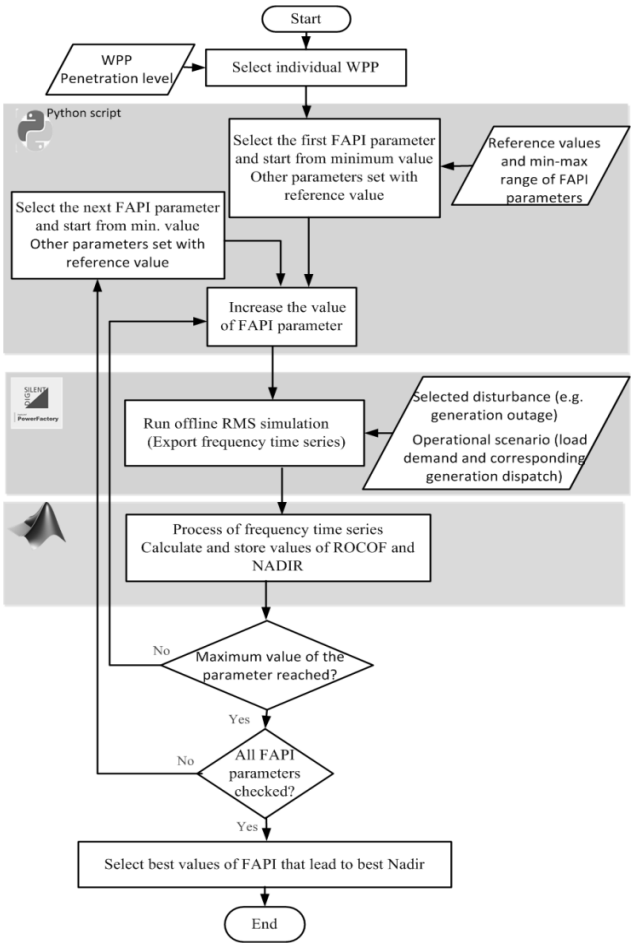

FIGURE 8. **Procedure for tuning of the FAPI control parameters.**

delivered power. For implementing this second-order function in PowerFactory the following equation is used:

$$\frac{P_o}{P_{in}} = \frac{1}{1 + K_z s + K_w s^2} = \frac{\frac{1}{K_w}}{s^2 + \frac{K_z}{K_w}s + \frac{1}{K_w}} \tag{4}$$

where $1/K_w = \omega_n^2$ and $K_z/K_w = 2\zeta\omega_n$.

IV. CONTROLLER TUNING

The FAPI controllers, explained in Section III, are evaluated to determine the possible increase of the share of PEIG that can be achieved in the grid without jeopardizing frequency stability.

The proposed sensitivity based approach for tuning the FAPI controller's parameters located in selected wind power plants are presented in Figure 8. This process will be used for a given test grid with several wind units for a given penetration level. For enabling this process the primary values of the FAPI control parameters for a given contingency, a given peak load with generation dispatches for a selected contingency, operational scenario and the network topology are necessary. According to the needs and priorities of system operators, different contingencies like the outage of the largest generator

TABLE 1. Parameters used for FAPI controllers.

Selected control parameters	Value
f_{th} [Hz]	49.90
f_p [Hz]	49.75
K_p [pu]	0.25
T_{imx} [s]	15
f_n [Hz]	50
K_d [pu]	10
T [s]	0.25
K_s [pu]	0.07
K_w [pu]	0.3

can be considered. Then, for each single wind generator which is facilitated with the FAPI controller, an automatic procedure (using the Python platform) is implemented to sweep over the parameters of the FAPI controller. As shown in Figure 8, a time-domain simulation can be executed for extracting time data series e.g. grid frequency, for more analysis in Matlab software. A Matlab script is used to evaluate the dynamics of the grid, e.g. calculation of Nadir for the selected operational scenario.

The main goal here is to find a set of suitable values for FAPI parameters which can improve the FFR capabilities of the WG. The automatic procedure is performed for tuning each single wind generation unit. After that, a new operational scenario with a higher share of wind power can be selected and re-tuned by applying the same iteration considering various combinations between the wind parks.

V. SIMULATION RESULTS WITH GB TEST SYSTEM

In this section, different FAPI controllers with their respective tuned parameters are analyzed in the GB test network. The RMS model of the GB test system is implemented to assess the impact of the FAPI controllers in providing the mitigation measures for determining the maximum achievable share of wind power generation in GB. The parameters of the FAPI controllers obtained after tuning are presented in Table 1. The studied operational scenario for the GB system, shown in Figure 1, is the Gone-Green 2030 with a different share of wind generation.

The fault is considered with the outage of the largest generation unit in the winter profile (G15) at 2 s.

It should be noted that, from an economic point of view, it is not necessary to facilitate all the wind parks with FAPI controller. The tuning procedure in Fig. 8 defined that FAPI should be installed in wind parks which are big enough for impacting the grid. Therefore, it is of interest to indicate the best combination of wind parks which are giving almost the same performance when all the wind parks are having FAPI.

After performing parametric sensitivity for the droop based FAPI controller, the best combination of wind power plants are presented in Figure 9. According to the obtained result, the selected combination (Figure 9) is C5.

This combination is shown in figure 1 and consists of WP9, WP10, WP16, WP19, and WP20. These wind parks

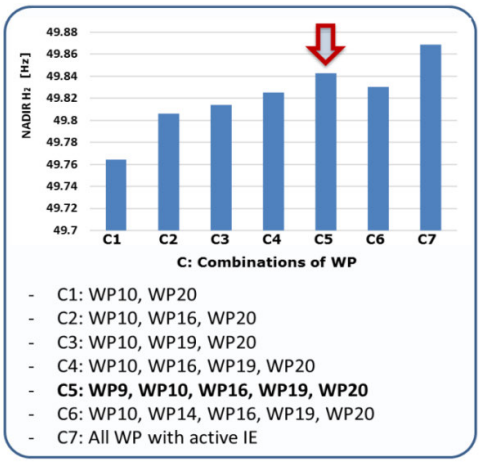

FIGURE 9. GB system with combinations of wind power plants.

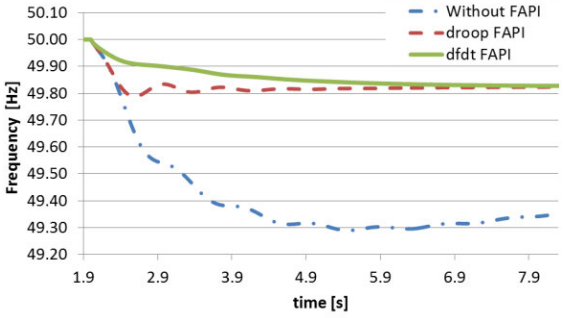

FIGURE 10. Frequency response for derivative-based FAPI (GB test system, 70% of the share of wind power generation).

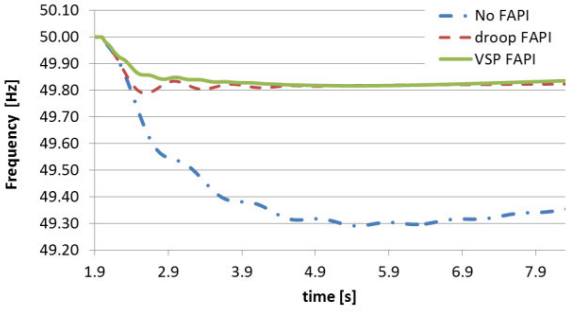

FIGURE 11. Frequency response for VSP-based FAPI (GB test system, 70% of the share of wind power generation).

are the largest units in the selected zones. Then, the testing of the proposed FAPI controllers is performed for scenario GG2030 with a high share of wind generation, i.e. around 70%.

A comparison between the system without FAPI and the system with different FAPI controls are presented in Figures 10 and 11.

It is worth mentioning that, in addition to the size, the location of wind turbines with FAPI and geographical situations

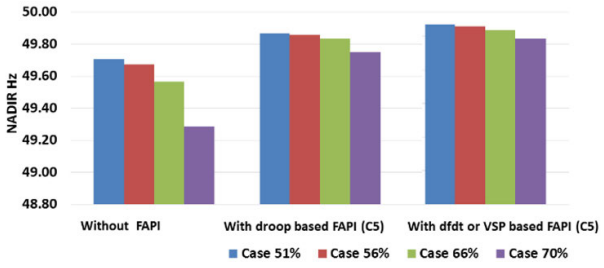

FIGURE 12. **Nadir values for a selected share of wind generation with and without FAPI controllers (GB test system).**

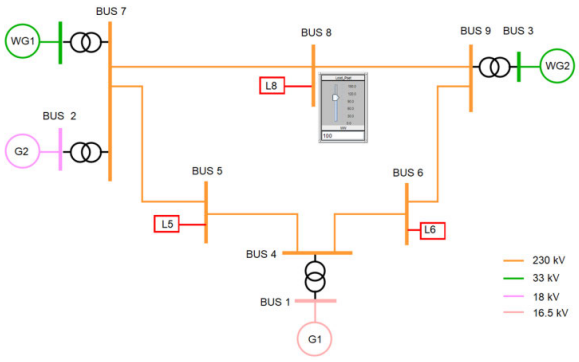

FIGURE 13. **Generic test case-2 with added WG.**

like wind speed might be an alternative criterion for impacting the dynamic performance of the system. According to the finding in [37], it is better to have the PEIG units in proximity to low-inertia regions and far from the center of inertia in the system. Furthermore, as reported in [38], when the wind speed is low, the contribution of FAPI controller (time duration and proportional gains) should be accordingly reduced in coherence with the available kinetic energy and if the speed is very low below rated operation, FAPI should not be activated to avoid stalling. Thus, it is worth evaluating if a minimum subset (combination) of wind power plants with FAPI can entail satisfactory frequency performance as in the case when all wind power plants perform with FAPI.

A. DERIVATIVE BASED CONTROLLER WITH THE GB SYSTEM

In this section, an analysis with a derivative-based FAPI controller is performed for the GB test system with scenario GG2030 and a higher share of wind generation (70%). A comparison between the system without FAPI and the system with droop-based and derivative-based FAPI controllers is presented in Figure 10. Therein, the obtained results demonstrate the dynamic improvements enabled by the derivative-based FAPI controller. The application of a derivative-based FAPI controller helps the system to achieve a better RoCoF and to mitigate oscillatory behavior.

B. VSP-BASED FAPI WITH THE GB SYSTEM

In this part of the study, the effect of the proposed VSP-based FAPI controller is analyzed by adding additional energy storage in the same location of the wind power plants.

According to Figure 9, the same combination (C5) with 70% penetration of the wind generation is used to assess the impacts of the proposed VSP-based FAPI controller.

The studied disturbance is the outage of G15, which covers around 5% of the total load on the system. A comparison of the frequency response is presented in Figure 11. The obtained results confirm the superiority of the VSP based FAPI controller compared to the droop based FAPI.

Finally, the effectiveness of the proposed derivate-based FAPI and VSP-based FAPI controllers for increasing the share of wind power generation is illustrated in Figure 12 (in terms of computed Nadir). According to Figure 12, thanks to the proposed FAPI approaches, the maximum achievable share of PEIG in the GB system can be increased up to 70% without violation from frequency limits defined by grid codes. It is worth mentioning that the technical limit on the allowable RoCoF and Nadir is system dependent, as reflected in the different grid codes of different TSOs. For instance, in Eirgrid the value for Nadir is around 48 Hz during disturbances (or 49.8 Hz in normal operation) with 0.5 Hz/s for RoCoF [39]. In the grid code of GB, the value for RoCoF is around 0.5 Hz/s for the situation with low inertia and the value for Nadir is around 49.5 Hz [40]. Considering the National Grid (NG) criterion, the limit for Nadir can be considered 49.8 Hz if the power mismatch is higher than 300 MW [36].

VI. VALIDATION WITH REAL-TIME SIMULATOR

This section presents the design and implementation of the controller by using an EMT test system build in a real-time digital simulator RTDS [41]. The test system is designed to represent specific critical situations, e.g. an operational scenario and electrical disturbance, which makes the system prone to frequency instability.

The EMT model of the interconnected power system is developed on RSCAD and running on RTDS NovaCor. RTDS allows external devices to be interfaced with the power system being simulated. The Software model for controlling the grid emulator and the device under test (DUT) was developed by Triphase in Matlab/ Simulink environment, which is running on a Real-Time Target (RTT) in real-time. RTT is a powerful, multi-core PC-based unit equipped with a real-time Linux/Xenomai-based operating system. A real-time inter-PC interface enables RTT to connect in real-time to the RTDS. The user has access and control on set-points of voltage and frequency of grid emulator and current set-points of DUT. RTT receives these set-points from RTDS. The Aurora communication protocol is used to exchange information between RTDS simulations and the RTT. The EMT test system is based on the IEEE 9-bus test System, which is modified by adding two averaged EMT models of the wind generator type 4 [34], which is a more detailed model of the RMS wind model shown in Fig. 2 [34]. The layout of the test system is shown in Figure 13. Table 2 describes the load flow results in pre-disturbance conditions.

TABLE 2. Load flow results from a test system with 52% wind share.

Load Flow Results		P (MW)	Q (MVAR)
Generations	G1	73.4	33.8
	WG1	82.6	0
	G1	78.2	-1.8
	WG2	84	0
Loads	L5	125	50
	L6	90	30
	L8	100	35

In this scenario, bus 8 was selected to create an under-frequency event (5% load increase at 1,5 sec) because the disturbance caused at this bus had the highest impact on Bus 3 and Bus 7, where the wind turbines are connected.

A. DERIVATIVE-BASED FAPI VALIDATION

Figure 14 depicts the frequency plots test obtained for various values of proportional (K_p) and derivative gains (K_d) in reference to the derivative-based FAPI controller. The values selected here are the possible combinations of K_p and K_d achieved by careful tuning. The values of K_p and K_d are not only system-dependent but also dependent on the grid to which the wind generators are connected along with the disturbance to which they are exposed.

Here the plot with $K_p = 0$ and $K_d = 0$, forms the base plot with no derivative controller action. With $K_p = 0.4$ and $K_d = 0.6$, it can be observed that since K_p value is less, Nadir improvement is comparatively less but considerable improvement in dynamic frequency response before Nadir can be observed. A comparison between plots of $K_p = 0.73$, $K_d = 0.65$ and $K_p = 0.73$, $K_d = 0.68$ depicts how sensitive the controller's behaviour is to the value of K_p and K_d and consequently, the latter case shows the issues with under-damping which brings the oscillatory effect.

At last, the plot with $K_p = 0.9$ and $K_d = 0.4$ gave the best results with RoCoF improvement from 280mHz/sec (base case) to 139.7mHz/sec accounting to 52% increase in RoCoF and Nadir shift from 49.64 Hz (base case) to 48.845 Hz accounting to 58.3% increase in Nadir. RoCoF is calculated for a time window of 500ms from 1.905 secs to 2.405 secs after the time of dead-zone (around 405ms).

In summary, with the derivative-based FAPI controller, both Nadir and dynamic frequency response before Nadir could be improved by careful tuning of controller gains.

B. COMPARISONS WITH VSP-BASED FAPI CONTROLLER

Figure 15(a) shows the comparison between the different FAPI control strategies that can be implemented in a type-4 wind generator. As explained in Section III, three different types of FAPI has been considered, droop based FAPI, derivative plus droop based FAPI and VSP based FAPI controller.

Form the obtained results it can be noticed that the best performance is from the VSP-based FAPI controller which improves both Nadir and RoCoF the highest, but this requires

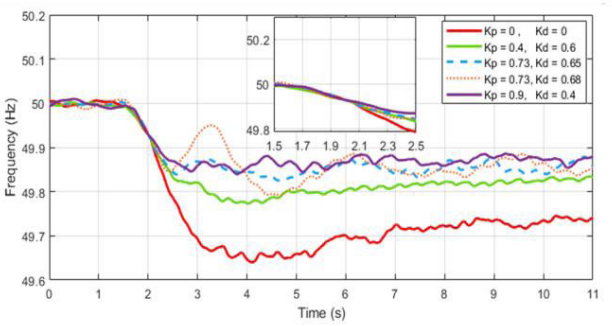

FIGURE 14. Frequency response due to load increase at bus 8 with derivative-based FAPI controller at WG's.

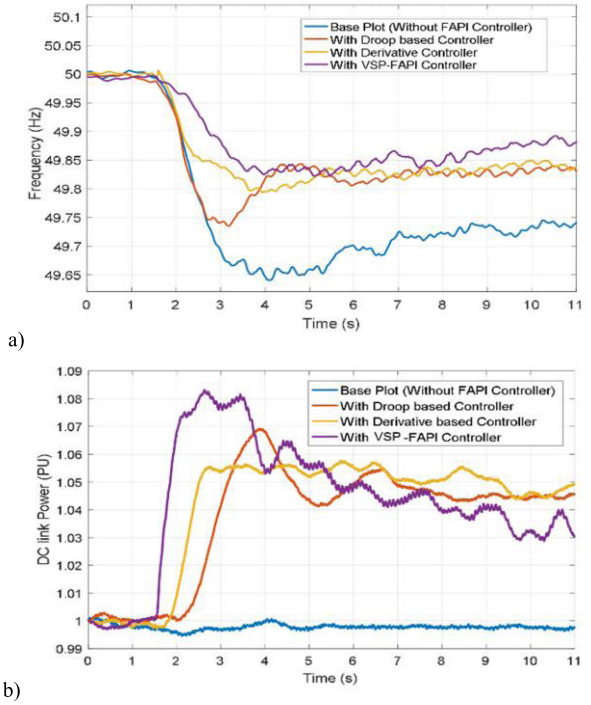

FIGURE 15. (a) Frequency response due to load increase at bus 8 with FAPI controller at WG's; (b) DC Link Power at the type 4 wind generator due to FAPI controllers.

an extra BESS or super-capacitor for injection of additional power. Figure 15(b) shows the comparison of the DC-link Power of a type-4 Wind generator due to different FAPI control strategies.

It is noticeable that, though triggering time is 1.5 s in all cases, the VSP-based FAPI controller has a response rate faster than other controllers due to two reasons, one being PLL less operation and the other being the fast characteristics of 2nd order transfer function used in VSP-based FAPI block.

Since the models considered in this part of the study were full scale, more details considering the limitations of FAPI controllers with realistic response behaviour close to real systems were tested. The following issues have to be considered:

- The DC-link Power cannot be increased beyond 10%, because of the limitation on VSC switches on the Grid side converter (inverter).

- The Battery considered in the RSCAD model is almost ideal since it does not take into consideration the electrochemical behaviour seen in the real system.

VII. CONCLUSION

Different forms of mitigation measures, namely droop-based FAPI, derivative-based FAPI, and VSP-based FAPI controllers, for enhancing the dynamics of the frequency of a low-inertia system in the containment period have been presented and later discussed.

A parametric sensitivity-based method for assessing the impacts of the FAPI controller settings was also proposed and applied in the GB test system. Based on the obtained results, it becomes clear that the fast delivery of a large amount of power is essential to quickly arrest the frequency deviations due to a large active power imbalance. This goal can be achieved by using the derivative or the VSP-based FAPI controls. Simulations conducted on the GB system showed that it is possible to increase the penetration level of the wind power to up to 70%, without violating the assumed threshold for Nadir. The VSP technique would be a preferred method due to the fact that it can be used for different functionalities, e.g. fast frequency control and oscillation damping, without any dependency on frequency estimation by the PLL.

Other findings from the application of different FAPI controllers are summarised as follows:

- According to TSO priorities and available sources of energy, the time duration for FAPI can be selected. The recommended range for the activation period is between 5 s to 30 s [21], [36] and [41].
- The proposed controller is an effective solution for frequency mitigation. In the modified controller (combined methods of proportional droop + derivative), both Nadir and RoCoF values can be improved.
- Depending on the available energy, according to the studies performed in this work, the derivative gain can vary from 5 to 15. Due to the amplification of high-frequency noises, it's advisable to avoid using high values for the derivative gain. A low pass filter with a time constant around 0.25 s can be used to lessen this limitation [22].
- Estimation of RoCoF as an input signal can help the performance of the frequency derivative-based FAPI controller. This can be confidently done by using emerging approaches, like the Kalman filter-based method [42].
- Since the source of energy for the modified controller is the mechanical part of the wind turbines, then its performance will be limited by its physical limits. This method can also be implemented by using energy storage systems to consider more flexibility.
- The proposed VSP-based FAPI implements the electromechanical closed-loop diagram of Figure 7 in the outer loop controller of a grid-connected VSC. Nevertheless, it should be noted that the main target of the VSP is not to fully imitate the dynamic response of a conventional SG (represented with high order model), but it can effectively recover the weaknesses of the inherent oscillatory response of the conventional SG by using a single set of parameters that lead to a suitable response whenever there is an active power imbalance in the system.
- In terms of the dynamic performance of the VSP, it is possible to simultaneously provide damping and inertia, without limitations from the PLL scheme in providing input signals to the FAPI controller.

ACKNOWLEDGMENT

This article reflects only the authors' views, and the European Commission is not responsible for any use that may be made of the information it contains.

REFERENCES

[1] A. Gomez-Exposito, A. J. Conejo, and C. Cañizares, *Electric Energy Systems: Analysis and Operation*. Boca Raton, FL, USA: CRC Press, 2008.
[2] E. Rakhshani and P. Rodriguez, "Active power and frequency control considering large scale RES," in *Large Scale Renewable Power Generation* (Advances in Technologies for Generation Transmission and Storage). Berlin, Germany: Springer, Nov. 2013.
[3] H. Gu, R. Yan, and T. K. Saha, "Minimum synchronous inertia requirement of renewable power systems," *IEEE Trans. Power Syst.*, vol. 33, no. 2, pp. 1533–1543, Mar. 2018.
[4] H. Mortazavi, H. Mehrjerdi, M. Saad, S. Lefebvre, D. Asber, and L. Lenoir, "A monitoring technique for reversed power flow detection with high PV penetration level," *IEEE Trans. Smart Grid*, vol. 6, no. 5, pp. 2221–2232, Sep. 2015.
[5] H. Mehrjerdi and E. Rakhshani, "Correlation of multiple time-scale and uncertainty modelling for renewable energy-load profiles in wind powered system," *J. Cleaner Prod.*, vol. 236, Nov. 2019, Art. no. 117644.
[6] E. Rakhshani, D. Remon, and P. Rodriguez, "Effects of PLL and frequency measurements on LFC problem in multi-area HVDC interconnected systems," *Int. J. Electr. Power Energy Syst.*, vol. 81, pp. 140–152, Oct. 2016.
[7] H. Mehrjerdi, A. Iqbal, E. Rakhshani, and J. R. Torres, "Daily-seasonal operation in net-zero energy building powered by hybrid renewable energies and hydrogen storage systems," *Energy Convers. Manage.*, vol. 201, Dec. 2019, Art. no. 112156.
[8] B. K. Poolla, D. Gros, and F. Dorfler, "Placement and implementation of grid-forming and grid-following virtual inertia and fast frequency response," *IEEE Trans. Power Syst.*, vol. 34, no. 4, pp. 3035–3046, Jul. 2019.
[9] A. Adrees, J. V. Milanović, and P. Mancarella, "Effect of inertia heterogeneity on frequency dynamics of low-inertia power systems," *IET Gener., Transmiss. Distrib.*, vol. 13, no. 14, pp. 2951–2958, Jul. 2019.
[10] E. Rakhshani, D. Gusain, V. Sewdien, J. L. R. Torres, and M. A. M. M. Van Der Meijden, "A key performance indicator to assess the frequency stability of wind generation dominated power system," *IEEE Access*, vol. 7, pp. 130957–130969, 2019.
[11] N. W. Miller, K. Clark, and M. Shao, "Frequency responsive wind plant controls: Impacts on grid performance," in *Proc. IEEE Power Energy Soc. Gen. Meeting*, Jul. 2011, pp. 1–8.
[12] P. Tielens and D. Van Hertem, "The relevance of inertia in power systems," *Renew. Sustain. Energy Rev.*, vol. 55, pp. 999–1009, Mar. 2016.
[13] M. H. Othman *et al.*, "Progress in control and coordination of energy storage system-based VSG: A review," *IET Renew. Power Gener.*, vol. 14, no. 2, pp. 177–187, Feb. 2020.
[14] X. Li, Z. Li, L. Guo, J. Zhu, Y. Wang, and C. Wang, "Enhanced dynamic stability control for low-inertia hybrid AC/DC microgrid with distributed energy storage systems," *IEEE Access*, vol. 7, pp. 91234–91242, 2019.
[15] C. Mosca *et al.*, "Mitigation of frequency stability issues in low inertia power systems using synchronous compensators and battery energy storage systems," *IET Gener., Transmiss. Distrib.*, vol. 13, no. 17, pp. 3951–3959, Sep. 2019.

[16] M. S. Uz Zaman, S. B. A. Bukhari, R. Haider, M. O. Khan, S. Baloch, and C.-H. Kim, "Sensitivity and stability analysis of power system frequency response considering demand response and virtual inertia," *IET Gener., Transmiss. Distrib.*, vol. 14, no. 6, pp. 986–996, Mar. 2020.
[17] M. Dreidy, H. Mokhlis, and S. Mekhilef, "Inertia response and frequency control techniques for renewable energy sources: A review," *Renew. Sustain. Energy Rev.*, vol. 69, pp. 144–155, Mar. 2017.
[18] F. Hafiz and A. Abdennour, "Optimal use of kinetic energy for the inertial support from variable speed wind turbines," *Renew. Energy*, vol. 80, pp. 629–643, Aug. 2015.
[19] S. Mishra, P. P. Zarina, and P. C. Sekhar, "A novel controller for frequency regulation in a hybrid system with high PV penetration," in *Proc. IEEE Power Energy Soc. Gen. Meeting*, Jul. 2013, pp. 1–5.
[20] W. Yao and K. Y. Lee, "A control configuration of wind farm for load-following and frequency support by considering the inertia issue," in *Proc. IEEE Power Energy Soc. Gen. Meeting*, Jul. 2011, pp. 1–6.
[21] S. Engelken, A. Mendonca, and M. Fischer, "Inertial response with improved variable recovery behaviour provided by type 4 WTs," *IET Renew. Power Gener.*, vol. 11, no. 3, pp. 195–201, Feb. 2017.
[22] E. Rakhshani and P. Rodriguez, "Inertia emulation in AC/DC interconnected power systems using derivative technique considering frequency measurement effects," *IEEE Trans. Power Syst.*, vol. 32, no. 5, pp. 3338–3351, Sep. 2017.
[23] F. Gonzalez-Longatt, E. Chikuni, and E. Rashayi, "Effects of the synthetic inertia from wind power on the total system inertia after a frequency disturbance," in *Proc. IEEE Int. Conf. Ind. Technol. (ICIT)*, Feb. 2013, pp. 826–832.
[24] T. Ackermann, *Wind Power in Power Systems Edited*, vol. 140, no. 1. London, U.K.: Wiley, 2005.
[25] E. Rakhshani, D. Remon, A. M. Cantarellas, J. M. Garcia, and P. Rodriguez, "Virtual synchronous power strategy for multiple power systems," *IEEE Trans. Power Syst.*, vol. 32, no. 3, pp. 1665–1677, May 2017.
[26] Q. Zhong, S. Member, and G. Weiss, "Synchronverters: Inverters that mimic synchronous generators," *IEEE Trans. Ind. Electron.*, vol. 58, no. 4, pp. 1259–1267, Apr. 2011.
[27] L.-R. Chang-Chien, W.-T. Lin, and Y.-C. Yin, "Enhancing frequency response control by DFIGs in the high wind penetrated power systems," *IEEE Trans. Power Syst.*, vol. 26, no. 2, pp. 710–718, May 2011.
[28] J. M. Mauricio, A. Marano, A. Gomez-Exposito, and J. L. M. Ramos, "Frequency regulation contribution through variable-speed wind energy conversion systems," *IEEE Trans. Power Syst.*, vol. 24, no. 1, pp. 173–180, Feb. 2009.
[29] Z. Miao, L. Fan, D. Osborn, and S. Yuvarajan, "Wind farms with HVDC delivery in inertial response and primary frequency control," *IEEE Trans. Energy Convers.*, vol. 25, no. 4, pp. 1171–1178, Dec. 2010.
[30] R. Eriksson, N. Modig, and K. Elkington, "Synthetic inertia versus fast frequency response: A definition," *IET Renew. Power Gener.*, vol. 12, no. 5, pp. 507–514, Apr. 2018.
[31] *Electricity Ten-Year Statement*, Electricity Transmission (National Grid), London, U.K., 2016.
[32] L. Shen, "Model integration and control interaction analysis of AC/VSC HVDC system," Ph.D. dissertation, Dept. Elect. Electron. Eng., Univ. Manchester, Manchester, U.K., 2015.
[33] *Wind Turbines—Part 27-1: Electrical Simulation Models Wind Turbines*, Standard IEC 61400-27-1, 2017.
[34] *MIGRATE Project, Type-3 and Type-4 EMT—Model Documentation*, Energynautics, Darmstadt, Germany, 2017.
[35] J. Morren, S. W. H. de Haan, W. L. Kling, and J. A. Ferreira, "Wind turbines emulating inertia and supporting primary frequency control," *IEEE Trans. Power Syst.*, vol. 21, no. 1, pp. 433–434, Feb. 2006.
[36] *Need for Synthetic Inertia (SI) for Frequency Regulation*, ENTSO-E, Brussels, Belgium, 2017.
[37] H. Pulgar-Painemal, Y. Wang, and H. Silva-Saravia, "On inertia distribution, inter-area oscillations and location of electronically-interfaced resources," *IEEE Trans. Power Syst.*, vol. 33, no. 1, pp. 995–1003, Jan. 2018.
[38] A. Nikolopoulou, "Wind turbine contribution to ancillary services under increased renewable penetration levels," M.S. thesis, Dept. Elect. Sustain. Energy, Delft Univ. Technol., Delft, The Netherlands, 2018.
[39] *EirGrid Grid Code, Version 7, CC8.2*, EIRGRID, Dublin, Ireland, Dec. 2018.
[40] *International Review of Frequency Control Adaptation*, DGA Consulting, Australian Energy Market Operator, Melbourne, VIC, Australia, 2016.
[41] B. Wang, X. Dong, Z. Bo, and A. Perks, "RTDS environment development of ultra-high-voltage power system and relay protection test," *IEEE Trans. Power Del.*, vol. 23, no. 2, pp. 618–623, Apr. 2008.
[42] A. K. Singh and B. C. Pal, "Rate of change of frequency estimation for power systems using interpolated DFT and Kalman filter," *IEEE Trans. Power Syst.*, vol. 34, no. 4, pp. 2509–2517, Jul. 2019.

ELYAS RAKHSHANI (Member, IEEE) was born in 1982. He received the B.Sc. degree in power systems and the M.Sc. degree in control systems in 2008 and 2004, respectively, and the Ph.D. degree in electrical engineering from the Technical University of Catalonia (UPC), Barcelona, Spain, in 2016.

From 2013 to 2016, he was a Junior Researcher with the Research Department, Abengoa Company, Seville, Spain, working on different projects related to modern power systems. He has been with IEPG Center, Delft University of Technology (TU Delft), since March 2017, working on European projects related to control and dynamic stability assessment of renewable/power electronic-based power grids. He is currently a Senior Power System Consultant at ABB Power Grids, Madrid, Spain. His research interests include power system generation control and dynamic stability, power converter applications in power systems, renewable energy integration, frequency control, and optimal intelligent control. He has been involved in several national and international projects and has published several scientific journal articles and conference papers.

Dr. Rakhshani served as a technical program committee member for different conferences in power and energy fields. He is also an associate editor for several journals, such as IET journals.

ARCADIO PERILLA received the B.S. degree in electrical power engineering from Universidad Simón Bolívar, Caracas, Venezuela, in 2012, and the M.S. degree from Université Lille 1–Sciences et Technologies, Villeneuve-d'Ascq, France, in 2015. He is currently pursuing the Ph.D. degree in expandable high voltage DC systems as a part of the research program of the COBRA-cable Project with the Delft University of Technology, Delft, The Netherlands. He has been a Guest Ph.D. Student with SINTEF Energy Research, Trondheim, Norway, and the Department of Energy Technology, Aalborg University, Denmark. His research interests include modeling and control of power electronics interfaced generation for power systems dynamic stability assessment, modular multilevel converters applications for power systems, and multiterminal high-voltage dc networks operation, control, and protection.

JOSÉ L. RUEDA TORRES (Senior Member, IEEE) was born in 1980. He received the Ph.D. degree in electrical engineering from the Universidad Nacional de San Juan, San Juan, Argentina, in 2009. He is currently pursuing the Habilitation (qualification) degree with the University of Duisburg–Essen, Essen, Germany. From 2003 to 2005, he worked in Ecuador in the fields of industrial control systems and electrical distribution networks operation and planning. From 2010 to 2014, he was a Post-Doctoral Research Associate with the Institute of Electrical Power Systems, University of Duisburg–Essen. He is an Associate Professor leading the Research Team on Stability, Control, and Optimization in the Department of Electrical Sustainable Energy, Intelligent Electrical Power Grids Section, Delft University of Technology, Delft, The Netherlands. His research interests include power system stability and control, power system operational planning and reliability, and probabilistic and artificial intelligence methods. He is a member of the Technical Committee on Power and Energy Systems of the International Federation of Automatic Control (IFAC), the Chairman of the IEEE PES Working Group on Modern Heuristic Optimization, and the Secretary of CIGRE JWG C4/C2.58/IEEE Evaluation of Voltage Stability Assessment Methodologies in Transmission Systems.

FRANCISCO M. GONZALEZ-LONGATT (Senior Member, IEEE) is currently a Full Professor of electrical power engineering with the Institutt for elektro, IT og kybernetikk, Universitetet i Sørøst-Norge, Norway. His research interest includes innovative (operation/control) schemes to optimize the performance of future energy systems. He has prolific research productivity, including several industrial research projects and consultancy worldwide. He is the author or an editor of several books (Spanish and English) and an associate editor of several journals with an impressive track record on scientific publications. He is a member of The Institution of Engineering and Technology (IET), U.K., and the International Council on Large Electric Systems (CIGRE). He received professional recognition as a Fellow of the Higher Education Academy (FHEA) in January 2014. He is the Vice-President of Venezuelan Wind Energy Association.

THIAGO BATISTA SOEIRO (Senior Member, IEEE) received the B.S. (Hons.) and M.S. degrees in electrical engineering from the Federal University of Santa Catarina, Florianópolis, Brazil, in 2004 and 2007, respectively, and the Ph.D. degree from the Swiss Federal Institute of Technology, Zürich, Switzerland, in 2012. During his master's and Ph.D. studies, he was a Visiting Scholar with Power Electronics and Energy Research Group, Concordia University, Montreal, QC, Canada, and the Center for Power Electronics Systems, Blacksburg, VA, USA. From 2012 to 2013, he was a Senior Engineer with the Power Electronics Institute, Federal University of Santa Catarina. From 2013 to 2018, he was a Senior Scientist with Corporate Research Center, ABB Switzerland Ltd., Baden, Switzerland. Since 2018, he has been an Assistant Professor with the DC Systems, Energy Conversion and Storage Group, Delft University of Technology, Delft, The Netherlands. His research interests include advanced power converters and dc system integration.

MART A. M. M. VAN DER MEIJDEN (Member, IEEE) received the M.Sc. degree in electrical engineering from the Eindhoven University of Technology, Eindhoven, The Netherlands, in 1981. From 1982 to 1988, he was with ASEA/ABB in the field of process automation. Over the last 30 years, he has been working with different Dutch utilities. Since 2003, he has been the Innovation Manager with TenneT TSO B.V., responsible for the development of the TenneT Vision 2030. Since 2011, he has been a Full Professor with the Department of Electrical Sustainable Energy, Faculty of Electrical Engineering Mathematics, and Computer Science, Delft University of Technology, Delft, The Netherlands. He has been involved in development initiatives as grid technology innovation, implementation of sustainable energy, new organizational strategies, and implementation of asset management. He joined and chaired several national and international expert groups.